

DOI: 10.1002/sml.200600579

Towards Nanoporous Membranes based on ABC Triblock Terpolymers

Alexandra Sperschneider, Felix Schacher, Marcel Gawenda, Larisa Tsarkova, Axel H. E. Müller,* Mathias Ulbricht, Georg Krausch, and Jürgen Köhler

Block copolymers represent an exciting class of complex materials as they self-assemble into highly regular structures of nanoscopic dimensions. When prepared as thin films, such structures can be used for a variety of applications including lithographic masks or nanoporous membranes. Reported here are nanostructures in thin films of structurally analogous polybutadiene-block-poly(2-vinyl pyridine)-block-poly(*tert*-butyl methacrylate) (BVT) and polystyrene-block-poly(2-vinyl pyridine)-block-poly(*tert*-butyl methacrylate) (SVT) triblock terpolymers, which are synthesized via sequential living anionic polymerization. The morphological behavior of annealed SVT and BVT films is investigated by scanning force and electron microscopies. The difference in the terpolymer composition results in the formation of an ordered perforated lamella phase in SVT films and hexagonally packed core/shell cylinders in BVT films. Further, the BVT films show high potential for the fabrication of composite membranes using track-etched poly(ethylene terephthalate) macroporous filters as a support.

Keywords:

- membranes
- polymerization
- self-assembly
- thin films
- triblock terpolymers

1. Introduction

The development of synthetic membranes has always been inspired by nature, in particular by the fact that selective transport through biological membranes is enabled by highly specialized macro- and supramolecular assemblies

based on and involved in molecular recognition. The success of membrane technology has already been impressively demonstrated for the first large-scale industrial processes, water purification by reverse osmosis, and blood detoxification by dialysis or ultrafiltration. The search for novel synthetic membranes, in particular those with higher transport selectivity, is still a significant challenge in this field. Currently, most of the membranes used are produced from organic polymers via phase-inversion methods, that is, a controlled phase separation of polymer solutions induced by nonsolvent addition, solvent evaporation, or temperature change.^[1,2] Many scientifically interesting, technically challenging, and commercially attractive separation problems cannot be solved with membranes using current techniques. Novel membranes with a higher chemical selectivity, for example, for isomers, enantiomers, or larger biomolecules, or with a selectivity that can be switched by an external stimulus or that can adapt to the environment and process conditions are required. In addition, minimizing the thickness of

[*] A. Sperschneider, Prof. L. Tsarkova, Prof. G. Krausch
Physikalische Chemie II, Universität Bayreuth
95440 Bayreuth (Germany)
F. Schacher, Prof. A. H. E. Müller
Makromolekulare Chemie II, Universität Bayreuth
95440 Bayreuth (Germany)
Fax: (+49) 921-553393
E-mail: Axel.Mueller@uni-bayreuth.de
M. Gawenda, Prof. M. Ulbricht
Technische Chemie II, Universität Duisburg-Essen
45117 Essen (Germany)
Prof. J. Köhler
Experimentalphysik IV, Universität Bayreuth
95440 Bayreuth (Germany)

the membrane barrier layer is essential. Approaches to develop synthetic “next-generation” membranes have been recently reviewed.^[3]

The potential of block copolymers with incompatible blocks for nanotechnology applications has been realized in the past decade and a considerable number of examples has been described in the literature.^[4] Nanoporous materials may be generated by the selective removal of one of the components from a self-assembled block copolymer. Through adjusting chain length, composition, and molecular architecture, these materials are able to exhibit pore sizes and topology of parent structures and they can therefore be employed as nanolithographic masks, templates, or even separation membranes. Lee et al. first reported a porous membrane-like structure from an ordered block-copolymer precursor.^[5] The generated porous films were characterized by using adsorption measurements as well as gravimetric and spectroscopic methods. Three years later, Smith and Meier showed that ozonolysis can effectively remove the polydiene component in polystyrene-*block*-polybutadiene (PS-BB) or polystyrene-*block*-polyisoprene (PS-PI) diblock copolymers without altering the structure of the uncrosslinked PS domains.^[6] In 2003, Sidorenko et al. used a mixture of a polystyrene-*block*-poly(4-vinyl pyridine) (PS-P4VP) diblock copolymer and 2-(4-hydroxybenzene-azo)-benzoic acid (HABA). Depending on the casting conditions, the annealing solvent, and polymer-analogous reactions, thin films with pores perpendicular to the surface could be generated.^[7] An elegant way to obtain nanoporous materials without the need for crosslinking or degradation steps was shown by Zalusky et al.^[8] Mesoporous polystyrene monoliths were prepared by hydrolytical removal of the polylactide block from a polystyrene-*block*-polylactide (PS-PLA) diblock copolymer. Pore sizes within this system were adjustable via the molecular weight of the diblock copolymer. Rather simple methods for alignment of the PLA cylinders were also presented.^[9] Nanoporous PS generated in this way has the solubility and thermal characteristics of bulk polystyrene homopolymer and any potential application of these materials that requires pore structure stability must work within these limitations.

A different approach was published by Ndoni et al. in 2003.^[10] Here the polydiene component of a diblock copolymer was not removed through ozonolysis but kept as matrix material. They report on the synthesis and radical crosslinking of polybutadiene-*block*-poly(dimethylsilane) (PB-PDMS) followed by removal of the silane compound through HF etching. Unfortunately, the morphology was strongly affected by the rather rigorous crosslinking conditions. When replacing polybutadiene by polyisoprene and performing the etching step with tetrabutylammonium fluoride (TBAF) instead of HF, Cavicchi et al. obtained better results.^[11] They report on the formation of porous PI monoliths from ordered, aligned, and crosslinked PI-PDMS. Structures and porosity were investigated with scanning electron microscopy (SEM) and small-angle X-ray spectroscopy (SAXS) measurements after removal of the silyl component with TBAF in THF. These experiments showed that nanoporous rubbers may be generated, having potential as

functionalizable porous materials through the remaining double bonds.

It was shown earlier that the microdomain structures in thin films of SVT triblock terpolymer show pronounced dependence on the film thickness.^[12] Among those, the perforated lamella (PL) morphology is the most suitable for the fabrication of novel composite membranes. It was demonstrated experimentally^[13–16] and in computational simulation^[17] that in thin films of cylinder-forming block copolymers the PL phase is stabilized by the strong surface fields. Moreover, the PL structure was successfully converted into a pH-responsive layer through the hydrolysis of the ester moiety of the PtBMA component.^[18] Furthermore, additional morphologies such as short standing cylinders or complex gyroid structures, which provide a complex but regular channel geometry, are potentially of great interest.

Despite the impressive microscopic, spectroscopic, and other characterization studies of the ordered porous morphologies based on di- or triblock copolymers, a direct demonstration of the membrane function, that is, permeability measurements or even a selective permeation controlled by the nanoporosity of the polymer film, is yet to be accomplished.

Here we demonstrate the effect of the triblock terpolymer composition on the resulting complex morphology in thin films of polystyrene-*block*-poly(2-vinyl pyridine)-*block*-poly(*tert*-butyl methacrylate) (SVT) and of polybutadiene-*block*-poly(2-vinyl pyridine)-*block*-poly(*tert*-butyl methacrylate) (BVT) triblock terpolymers. Additionally, we varied the nature of the substrate, the molecular weight of the BVT terpolymer and the annealing conditions. By replacing the rather brittle polystyrene block in the SVT terpolymer through rubbery polybutadiene, we optimize the matrix properties, yielding a more flexible system. Furthermore, crosslinking of the polybutadiene compartment enhances the thin-film stability. The morphological behavior of annealed SVT and BVT films was investigated by scanning force microscopy (SFM), transmission electron microscopy (TEM) and SEM. The strategic aim of this work is to explore the potential of the fabrication of composite membranes from nanoporous block-copolymer thin films on macroporous filters as supports.

2. Results and Discussion

In order to induce long-range order of microstructures of block-copolymer thin films, thermal or solvent annealing procedures are typically applied. The assembly of microdomains at the microscale is accompanied by macroscale surface roughening, that is, the formation of terraces (coexisting flat regions with equilibrium film thickness) and of dewetting patterns. These two other dynamic processes are considered to pronouncedly and destructively affect (in case of dewetting) thin films from block copolymers with a relatively low total molecular weight. Thin polymer films consisting of comparatively long chains (with a total molecular weight above 100 kg mol^{-1}) are relatively stable towards dewetting^[22] on an experimental timescale. In addition, in

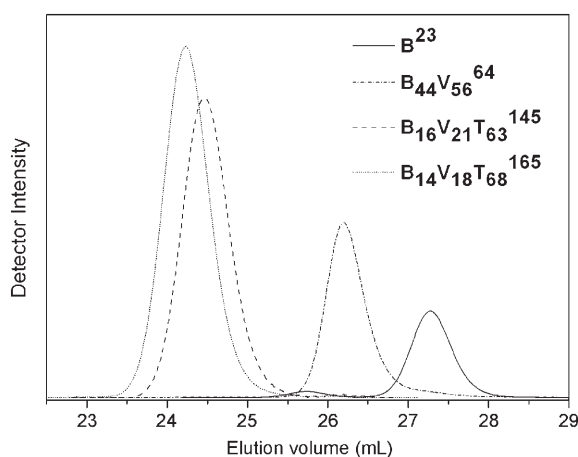


Figure 1. Gel permeation chromatography (GPC) eluograms of polybutadiene, polybutadiene-*b*-poly(2-vinyl pyridine), and two BVT tri-block terpolymers.

thin films of high-molecular-weight block copolymers, such as presented in this study, the terrace formation is considerably retarded due to the high viscosity of the polymers.^[23]

2.1 Thin-Film Phase Behavior of $S_{16}V_{21}T_{63}^{140}$.

After spin-casting from a chloroform solution, the samples were annealed for 100 h in chloroform vapor ($p_{\text{CHCl}_3} = 0.8p_0$, where p_0 represents the vapor pressure of chloroform at 295 K). Under these annealing conditions the polymer volume fraction in swollen films is $\phi = 0.36 \pm 0.04$. Due to the polymer swelling, the chain mobility is considerably increased, facilitating the diffusion-driven transport and the development of the equilibrium macro- and microstructures.

The annealed $S_{16}V_{21}T_{63}^{140}$ samples show macrostructures (terraces) on a scale of tens of micrometers (visible in optical microscopy). Large-scan SFM height images (not shown here) reveal coexisting terraces with the heights of $T_0 = 16 \pm 3$ nm and $T_1 = 36 \pm 2$ nm with characteristic microstructures in each terrace, which can only be visualized using SEM (Figure 2). On a microscale the SFM height and phase images show no lateral structure (inset in Figure 2A). The whole polymer surface is covered with a smooth, stiff layer of one component. In contrast, SEM measurements show the surface layer to be unstable during the electron-beam exposure despite a low acceleration voltage of 0.5 kV. Comparing all three polymer components, poly(*tert*-butyl methacrylate) (PtBMA) is the only block that is depolymerized via photolysis during UV or electron-beam exposure.^[24] In addition, PtBMA represents the phase with the lowest surface tension (see Table 1), which is expected to form a glassy (glass-transition tem-

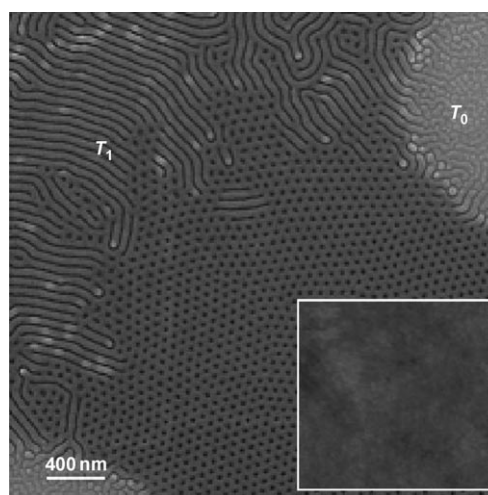


Figure 2. SEM image of a $S_{16}V_{21}T_{63}^{140}$ thin film after annealing in chloroform vapor ($p_{\text{CHCl}_3} = 0.8p_0$, $t = 100$ h) with an acceleration voltage of 1.0 kV showing different morphologies dependent on terrace height. Scale bar: 400 nm. Inset: SFM height image (size $1 \times 1 \mu\text{m}^2$; height scale $\Delta z = 0\text{--}20$ nm). The sample surface is covered with a smooth rigid layer of PtBMA.

perature $T_{g,(\text{PtBMA})} = 135^\circ\text{C}$) continuous cover layer that then minimizes the interfacial tension between the polymer film and air.^[25,26] The other two components, polystyrene ($\gamma_{\text{PS}} = 41 \text{ mN m}^{-1}$)^[27] and poly(2-vinyl pyridine) ($\gamma_{\text{P2VP}} = 40 \text{ mN m}^{-1}$)^[28], remain underneath this surface layer independent of the resulting morphology.

We now describe in more detail the microdomain structures as revealed by the SEM measurements. The thinnest part of the film (T_0 in Figure 1) is often referred to as a disordered phase or wetting layer. With increasing film thickness, T_0 transforms into cylinders orientated parallel to the substrate, which form the first terrace, T_1 . Moreover, with further increase of the film thickness to 47 ± 2 nm the cylindrical structure changes to PL morphology, resembling a typical filter or membrane surface. The associated changes in height within one terrace may be due to different characteristic spacings of the cylinders and the PL morphology.^[14] The molecular architecture of SVT suggests that a PL unit cell consists of a polystyrene core surrounded by a poly(2-vinyl pyridine) shell and penetrated by well-defined PtBMA pores (for further information see Refs. [12,13,31]). The SEM image of a $S_{16}V_{21}T_{63}^{140}$ thin film in Figure 3A indicates the formation of the PL phase over macroscopically large areas. The hexagonal order of perforations (pores) with an average diameter of 35 ± 3 nm is confirmed by the

Table 1. Surface tensions of polymer components.

Polymer	Surface tension [mN m^{-1}]
polystyrene	41.0 ^[27]
polybutadiene	24.5–32.0 ^[29,30]
poly(2-vinyl pyridine)	40.0 ^[28]
poly(<i>tert</i> -butyl methacrylate)	30.5 ^[27]

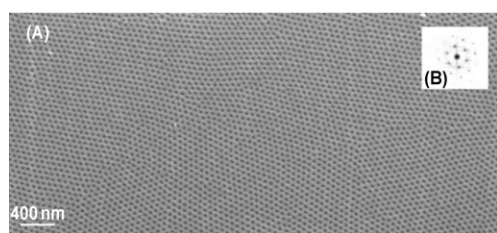


Figure 3. A) Typical SEM image of a $S_{16}V_{21}T_{63}^{140}$ triblock terpolymer thin film after spin-casting from chloroform solution and solvent annealing for 100 h; acceleration voltage 1.0 kV. Scale bar: 400 nm. B) Fourier transformation confirms the hexagonally arranged PL structure.

Fourier transformation (inset of Figure 3 B). The estimated porosity of such nanostructures is about 21%. We note that the observed microstructures and terrace heights are in agreement with the combinatorial studies of Ludwigs et al.^[31]

2.2 Thin-Film Phase Behavior of $B_{16}V_{21}T_{63}^{145}$.

Spin-cast 30 ± 2 -nm-thick films were annealed in chloroform vapor under the same conditions as described for $S_{16}V_{21}T_{63}^{140}$. SFM height measurements reveal a macroscopically smooth surface of the film with no terraces formed upon the annealing procedure. On a smaller scale, the lateral nanostructures become visible.

The SFM height image in Figure 4 A reveals coexisting morphology represented by channels (dark and white stripes) and by wells (dark dots) surrounded by meshlike walls (bright area). In the corresponding phase image (Figure 4 B), two phases with different mechanical properties are clearly distinguished. The dark color in the phase image corresponds to the PB block, which is the only soft component in the presented system. The meshlike hard matrix is presumably composed of the two other glassy components, that is, P2VP and PtBMA. We note that, in contrast to the $S_{16}V_{21}T_{63}^{140}$ films, the PL morphology was not observed.

The nanostructured, free surface of $B_{16}V_{21}T_{63}^{145}$ films, as revealed by SFM measurements, indicates that PtBMA does not form the continuous surface layer that was detected for $S_{16}V_{21}T_{63}^{140}$ films (inset to Figure 1). This effect can be explained by the modified polymer composition, the consequential changes in T_g and the surface tension (Table 1) of the BVT components. Both PB and PtBMA blocks show comparable surface tension enabling both components to segregate to the free surface. Therefore, the lateral nanopattern can be resolved in solvent-annealed films by SFM measurements.

Additional information concerning the composition of the meshlike hard matrix was obtained by SEM. Figure 5 displays the microdomain pattern of the $B_{16}V_{21}T_{63}^{145}$ film described above (Figure 4). The structure is represented by core/shell stripes and dots, which we identify with the core/shell cylinders oriented parallel and perpendicular to the

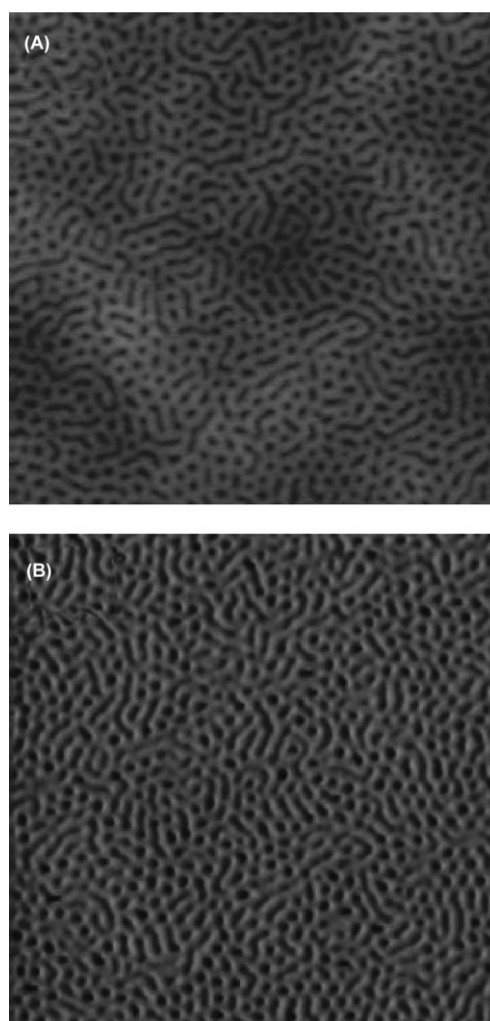


Figure 4. A) Typical SFM height image of a $B_{16}V_{21}T_{63}^{145}$ triblock terpolymer thin film spin-cast from chloroform solution after annealing for 100 h in chloroform vapor (image size $2.5 \times 2.5 \mu\text{m}^2$; height scale $\Delta z = 0\text{--}20$ nm) showing coexisting morphologies. The low, dark areas correspond to the soft PB compartment, which is distorted due to strong SFM tapping conditions. The higher, brighter meshlike matrix is presumably composed of the other two rigid polymer compartments P2VP and PtBMA. The contrast differences in the corresponding phase image (B) confirm this observation (image size $2.5 \times 2.5 \mu\text{m}^2$; phase contrast 30°).

film surface, respectively, with an average diameter of 67.8 ± 9.0 nm (Figure 5). The meshlike hard matrix, which was clearly visualized in SFM images (Figure 4), is decomposed upon electron-beam exposure, which implies that it is composed of PtBMA.

The stripes and distorted dots, which appear as defects in the hexagonally ordered structure of perpendicular cylinders, annihilate upon increasing the time of equilibration. Using a step-wise annealing process, we followed the evolution of cylinders lying parallel to the substrate into cylinders oriented perpendicular to the substrate. The TEM image in Figure 6 displays the mechanism of such a transformation via interfacial undulations along the parallel cylinder axis and the resulting breakup into spherical domains.^[32]

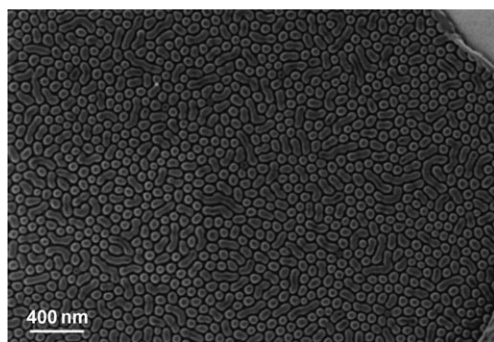


Figure 5. SEM image of the $B_{16}V_{21}T_{63}^{145}$ film shown in Figure 4 (acceleration voltage 0.5 kV). Only cylinders oriented perpendicular and parallel to the substrate surface are found, whereas the surrounding matrix phase, which was clearly resolved in the SFM height measurements (Figure 2), is depolymerized by the electron beam. Scale bar: 400 nm.

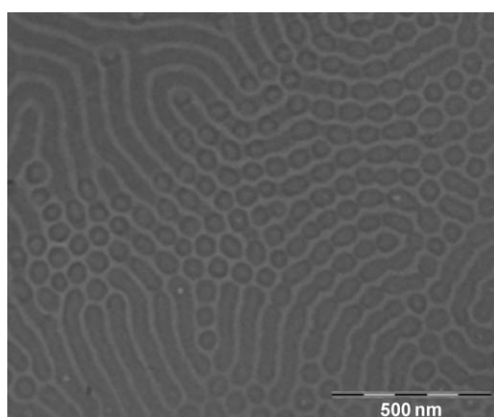


Figure 6. TEM image of a $B_{16}V_{21}T_{63}^{145}$ thin film successfully transferred after controlled solvent annealing for two hours reveals an intermediate stage in the cylinder-transformation mechanism. The cylinders orientated parallel to the substrate show a rather undulating shape resulting in a breakup into spherical domains. Scale bar: 500 nm.

2.3 Thin-Film Phase Behavior of $B_{14}V_{18}T_{68}^{165}$.

To further investigate the molecular architecture effects on the resulting morphology and long-range order, we studied a BVT terpolymer with increased total molecular weight. A 39 ± 3 -nm-thick film was prepared under the conditions described above. SFM height measurements revealed a smooth, macroscale film surface (no terrace development).

SEM measurements (not shown) reveal vertically oriented core/shell cylinders with an average diameter of 64 ± 5 nm, which look similar to the structures described above for $B_{16}V_{21}T_{63}^{145}$ films (Figure 5). In order to obtain further insight into the microdomain structure, we performed SFM measurements of the BVT films after exposure to the electron beam in SEM.

SFM height and phase images in Figure 7 clearly confirm the core/shell morphology. We note that due to removal of the PzBMA block, in the height image the film surface

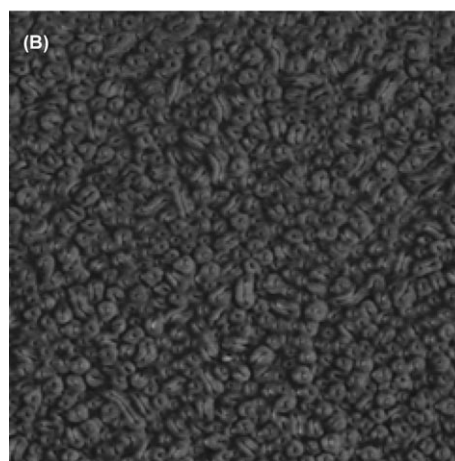
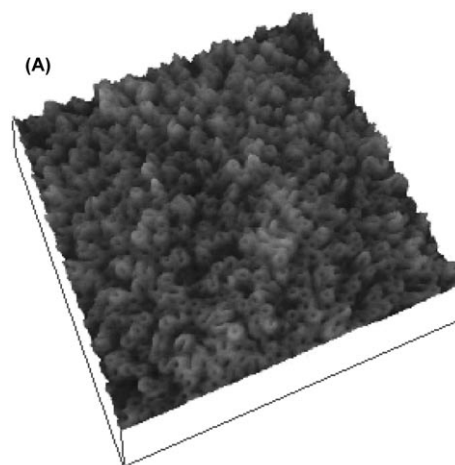


Figure 7. A) Typical three-dimensional SFM height image (image size $2.5 \times 2.5 \mu\text{m}^2$; height scale $\Delta z = 0\text{--}20$ nm) of a $B_{14}V_{18}T_{68}^{165}$ triblock terpolymer (spin-cast from chloroform solution, solvent annealed for 100 h) after electron-beam exposure. The resulting morphology of vertical cylinders can be easily observed. The corresponding phase image (B) confirms the structure of core/shell cylinders whereas the soft PB compartment forms the core (black area) and the stiff P2VP compartment equals the surrounding shell (bright area; image size $2.5 \times 2.5 \mu\text{m}^2$; phase contrast = 20°).

appears to be rough with an average roughness of 6 ± 1 nm, as calculated by the Nanoscope software. In order to probe the potential of BVT nanostructures in membrane technology, we replaced the silicon oxide substrate by the crystalline sodium chloride (NaCl) surface, which makes the transformation of the polymer film from the solid substrate for further analysis and usage more feasible. Immediately after annealing on the NaCl substrate, BVT films were transferred onto carbon-coated TEM grids. Carbon coating enhances film stability during electron-beam exposure.

The TEM image in Figure 8A clearly reveals the core/shell morphology, which confirms the successful film transfer. A further step towards optimization of the mechanical properties and chemical stability of the membrane prototypes was achieved by selective crosslinking of the PB component via UV initiator. The above procedure considerably improves the physical properties of the liquid polybutadiene

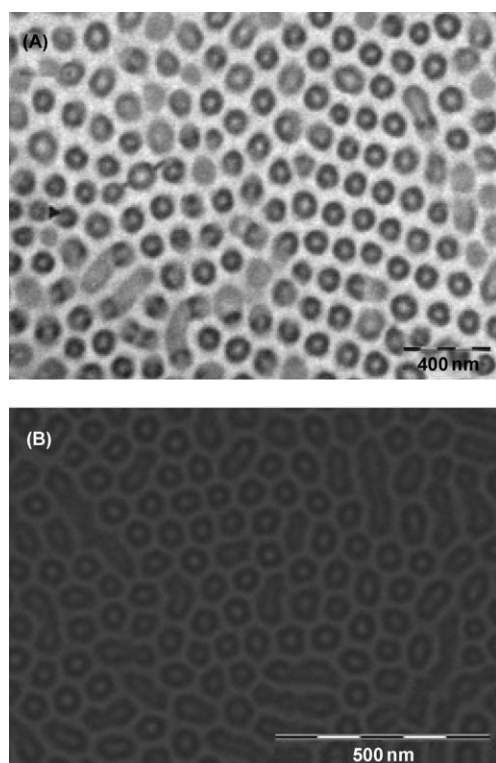


Figure 8. A) TEM image of a thin film of $B_{14}V_{18}T_{68}^{165}$ triblock terpolymer spin-cast onto a NaCl wafer from chloroform solution and transferred onto a TEM grid, revealing hexagonally packed core/shell cylinders: polybutadiene core and poly(2-vinyl pyridine) shell in a poly(*tert*-butyl methacrylate) matrix. Scale bar: 200 nm. B) TEM image of a crosslinked $B_{14}V_{18}T_{68}^{165}$ thin film displaying comparable structures as shown in (A). Scale bar: 500 nm.

segments, leading to a rubbery material and therefore facilitates the film transfer to the technologically approved substrates. Importantly, the desired film nanostructure is perfectly preserved after crosslinking (Figure 8B).

In order to characterize and probe the size/charge-based permeation selectivity of block copolymer nanostructures, thin polymer films must be transformed onto suitable substrates providing sufficient mechanical stability of a potential membrane. Considering the diameters of the pore precursors identified in this work (≈ 35 nm; SVT), moderately thick (membrane) filters with pore diameters of between ≈ 0.2 and ≈ 5 μm are suitable base materials for the fabrication of block-copolymer thin-film composite membranes. Surface-functionalized track-etched poly(ethylene terephthalate) (PET) membranes, which have already been well established as model systems for selective and stimuli-responsive transport through well-defined pores in the nano- and micrometer range,^[3,33] are the first choice. The transfer onto other supports, for example to silicon nitride-based microsieves,^[34] is another perspective. The results of our study demonstrate that upon annealing under sufficient solvent vapor pressure, the resulting microdomain structure is not sensitive to the chemical nature of the substrate (NaCl or silicon oxide) due to the strong screening effect of the solvent. On the other hand, the transfer of the polymer films

to the supporting membranes is considerably facilitated by the improved mechanical properties of the films.

3. Conclusions

SFM, TEM, and SEM reveal the nanostructures in thin films of structurally analogous polybutadiene-*block*-poly(2-vinyl pyridine)-*block*-poly(*tert*-butyl methacrylate) (BVT) and polystyrene-*block*-poly(2-vinyl pyridine)-*block*-poly(*tert*-butyl methacrylate) (SVT) triblock terpolymers. The difference in the terpolymer composition results in the formation of an ordered perforated-lamella phase in SVT films and hexagonally packed core/shell cylinders in BVT films. Both morphologies are considered to be attractive precursors for nanoporous separation membranes. This requires further processing of the films via selective degradation of one component in order to “open” the pores.

For the novel BVT terpolymers, several very useful features with respect to the membrane technology have been identified, namely, a similar equilibrium morphology on substrates with different wettability, the feasibility of film transfer to another (porous) substrate, and the stabilization of the films by internal crosslinking. Thin SVT films demonstrated membrane-suitable morphology and feasibility of their transfer onto support membranes. Further processing of terpolymer microstructures towards nanoporous separation membranes is currently under investigation.

4. Experimental Section

Synthesis of block terpolymers: The synthesis and characterization of the linear SVT triblock terpolymers have already been described.^[19] The BVT triblock terpolymers were synthesized via sequential living anionic polymerization in THF using *sec*-butyl lithium as initiator. After polymerization of butadiene and 2-vinyl pyridine at -10 °C and -70 °C respectively, 1,1-diphenylethylene was added to reduce the nucleophilicity of the living chain ends. During the polymerization of the PtBMA block at -35 °C, samples were taken from the reactor after different polymerization times and were precipitated into degassed methanol. The number-average molecular weight of the polybutadiene precursor and the molecular-weight distributions of the triblock terpolymers were determined by gel permeation chromatography (GPC). All polymers exhibit a narrow molecular-weight distribution characterized by polydispersity indices between 1.01 and 1.05. Additionally, ^1H NMR spectra were acquired using CDCl_3 as solvent and tetramethylsilane (TMS) as internal standard. The molecular weights of the P2VP and the PtBMA blocks were calculated using the terpolymer composition determined by NMR and the polystyrene molecular weights from GPC. The molecular parameters of the triblock terpolymers are listed in Table 2 and GPC eluograms of BVT are shown in Figure 1.

Size-exclusion chromatography (SEC): SEC measurements were performed on a set of 30-cm SDV-gel columns of 5- μm particle size and with nominal pore sizes of 10^5 , 10^4 , 10^3 , and

Table 2. Molecular characteristics of triblock terpolymer.

Polymer ^[a]	M_w/M_n ^[b]	$\Phi_{PS/PB}:\Phi_{P2VP}:\Phi_{PtBMA}$ ^[c]
S ₁₆ V ₂₁ T ₆₃ ¹⁴⁰	1.03	1 : 1.3 : 3.90
B ₁₆ V ₂₁ T ₆₃ ¹⁴⁵	1.02	1 : 1.3 : 3.90
B ₁₄ V ₁₈ T ₆₈ ¹⁶⁵	1.02	1 : 1.3 : 4.85

[a] Subscripts represent the weight fractions of the respective block (in weight%); the superscript denotes the total weight-average molecular weight in kg mol⁻¹. [b] Polydispersity determined by GPC. M_w = weight-average molecular weight; M_n = number-average molecular weight. [c] Relative volume fractions of blocks.

10² Å with refractive index and UV (λ = 254 nm) detection. An elution rate of 1 mL min⁻¹ with THF as solvent was used.

¹H NMR: ¹H NMR spectra were recorded on a Bruker 250 ac spectrometer using either CDCl₃ or [D₆]THF as solvent and tetramethylsilane (TMS) as internal standard.

Thin-film preparation: SVT and BVT polymer thin films were prepared by spin-casting 5 g L⁻¹ solutions in chloroform onto polished silicon wafers and NaCl surfaces, respectively. In order to improve the chain mobility and equilibrate the microdomains, the thin films were annealed under controlled solvent vapor pressure. The samples were subsequently quenched by a flow of pure dried air in order to freeze the developed morphologies. The fast quenching procedure ensures reproducibility.

For crosslinking of the polybutadiene block in BVT thin films, 3 wt.% of the photoinitiator Lucirin-TPO (BASF) was added to a 5 g L⁻¹ polymer solution. After spin-casting onto NaCl (crysTec GmbH, Germany) and annealing in controlled solvent vapor, the samples were subsequently exposed to UV light for 60 min with a cutoff at 300 nm, leaving the PtBMA block undamaged.

SFM: Microdomain structures and film thickness were investigated with SFM (Dimension 3100, Veeco Metrology) operated in tapping mode. The spring constant of the silicon cantilevers was in the range of 35–92 nN m⁻¹. The corresponding resonance frequency varied between 285 and 385 kHz. Phase images were recorded at free amplitudes of about 30–50 nm at a setpoint of 90% of the free cantilever amplitude. Height measurements were performed by scratching the polymer films with a scalpel (see Ref. [20]) and measuring the height of the polymer film surface with respect to the underlying substrate. The phase contrast was resolved due to the different physical properties of the components. Polybutadiene is liquid at room temperature whereas poly(*tert*-butyl methacrylate) and poly(2-vinyl pyridine) are in a glassy state at temperatures below 100 °C.

Field-emission SEM: We used SEM (LEO 1530, Zeiss) for further characterization of the polymer thin films. Due to the depolymerization of the PtBMA matrix phase by the electron beam, new insights into the morphology were gained.^[21] Applying the InLens detector with a slow acceleration voltage of 0.5 kV, we obtained a sufficient material contrast between the two remaining polymer phases without staining or sputtering.

TEM: To create new polymer-composite membranes, it is essential to remove the triblock terpolymers from the substrates, enabling the transfer to template membranes. To this end we prepared thin films of B₁₄V₁₈T₆₈¹⁶⁵ on NaCl substrates (as explained above). After solvent annealing, the NaCl plates were dissolved in bidistilled water and the free-floating film was

picked up with carbon-coated copper grids (Plano, Wetzlar). Subsequently, the samples were checked with TEM (CEM 902, Zeiss, 80 kV) for defects caused by the transfer.

Acknowledgements

This research is supported by the VolkswagenStiftung. We thank Carmen Kunert for the TEM measurements.

- [1] M. Mulder, *Basic Principles of Membrane Technology*, Vol. 2, Kluwer Academic Publishers, Dordrecht, The Netherlands, **1996**.
- [2] P. van de Witte, P. J. Dijkstra, J. W. A. van den Berg, J. Feijen, *J. Membr. Sci.* **1996**, *117*, 1.
- [3] M. Ulbricht, *Polymer* **2006**, *47*, 2217.
- [4] M. A. Hillmyer, *Nanoporous Materials from Block-Copolymer Precursors*, Vol. 189, Springer, Berlin, **2005**.
- [5] J. S. Lee, A. Hirao, S. Nakahama, *Macromolecules* **1988**, *21*, 274.
- [6] D. R. Smith, D. J. Meier, *Polymer* **1992**, *33*, 3777.
- [7] A. Sidorenko, I. Tokarev, S. Minko, M. Stamm, *J. Am. Chem. Soc.* **2003**, *125*, 12 211.
- [8] A. S. Zalusky, R. Olayo, C. J. Taylor, M. A. Hillmyer, *J. Am. Chem. Soc.* **2001**, *123*, 1519.
- [9] A. S. Zalusky, R. Olayo, J. H. Wolf, M. A. Hillmyer, *J. Am. Chem. Soc.* **2002**, *124*.
- [10] S. Ndoni, M. Vigild, R. H. Berg, *J. Am. Chem. Soc.* **2003**, *125*, 13 366.
- [11] K. A. Cavicchi, A. S. Zalusky, M. A. Hillmyer, T. P. Lodge, *Macromol. Rapid Commun.* **2004**, *25*, 704.
- [12] S. Ludwigs, G. Krausch, R. Magerle, A. V. Zvelindovsky, G. J. A. Sevink, *Macromolecules* **2005**, *38*, 1859.
- [13] S. Ludwigs, A. Böker, N. Rehse, A. Voronov, R. Magerle, G. Krausch, *Nat. Mater.* **2003**, *2*, 744.
- [14] L. Tsarkova, A. Knoll, G. Krausch, R. Magerle, *Macromolecules* **2006**, *39*, 3608.
- [15] I. Park, S. Park, H. W. Park, T. Chang, H. Yang, C. Y. Ryu, *Macromolecules* **2006**, *39*, 315.
- [16] A. Knoll, A. Horvat, K. S. Lyakhova, G. Krausch, G. J. A. Sevink, A. V. Zvelindovsky, R. Magerle, *Phys. Rev. Lett.* **2002**, *89*, 035 501.
- [17] D. A. Hajduk, *Macromolecules* **1997**, *30*, 3788.
- [18] S. Ludwigs, K. Schmidt, G. Krausch, *Macromolecules* **2005**, *38*, 2376.
- [19] S. Ludwigs, A. Böker, V. Abetz, A. H. E. Mueller, G. Krausch, *Polymer* **2003**, *44*, 6815.
- [20] L. Tsarkova, A. Knoll, G. Krausch, R. Magerle, *Macromolecules* **2006**, *39*, 3608.
- [21] L. C. Sawyer, D. T. Grubb, *Polymer Microscopy*, Chapman and Hall, London, **1996**.
- [22] M. Geoghegan, G. Krausch, *Prog. Polym. Sci.* **2002**, *28*, 261.
- [23] L. Tsarkova, in *Nanostructured Soft Matter: Experiment, Theory, Simulation, and Perspectives* (Ed.: A. V. Zvelindovsky), Springer Verlag, Heidelberg, **2007**.
- [24] N. Grassie, G. Scott, *Polymer Degradation and Stabilisation*, Cambridge University Press, Cambridge, UK, **1988**.
- [25] S. H. Anastasiadis, T. P. Russell, S. K. Satija, C. F. Majkrzak, *Phys. Rev. Lett.* **1989**, *62*, 1852.
- [26] H. Hasegawa, K. Hashimoto, *Macromolecules* **1985**, *18*, 589.
- [27] J. E. Mark, *Physical Properties of Polymers Handbook*, AIP Press, Woodbury, USA, **1996**.
- [28] K. Ishizu, Y. Yamada, T. Fukutomi, *Polymer* **1990**, *31*, 2047.

- [29] A. Turturro, E. Gattiglia, P. Vacca, G. T. Viola, *Polymer* **1995**, *36*, 3987.
- [30] L. H. Lee, *J. Polym. Sci. A-2* **1967**, *5*, 1103.
- [31] S. Ludwigs, K. Schmidt, C. M. Stafford, E. J. Amis, M. J. Fasolka, A. Karim, R. Magerle, G. Krausch, *Macromolecules* **2005**, *38*, 1850.
- [32] L. Tsarkova, A. Knoll, R. Magerle, *Nano Lett.* **2006**, *6*, 1574.
- [33] C. Geismann, A. Yaroshchuk, M. Ulbricht, *Langmuir* **2007**, *23*, 76.
- [34] C. J. M. Van Rijn, *Nano and Microengineered Membrane Technology*, Elsevier Science, Amsterdam, **2004**.

Received: October 19, 2006
Revised: March 13, 2007
Published online on April 20, 2007